A Highly Selective and Multisignaling Optical−Electrochemical Sensor for Hg^{2+} Based on a Phosphorescent Iridium(III) Complex

Qiang Zhao, Tianye Cao, Fuyou Li,* Xianghong Li, Hao Jing, Tao Yi, and Chunhui Huang*

Department of Chemistry & Laboratory of Advanced Materials, Fudan University, Shanghai, 200433, People's Republic of China

Received November 8, 2006

A highly selective phosphorescent chemosensor for Hg^{2+} based on the iridium(III) complex $Ir(btp)_2$(acac) was realized. Multisignaling changes were observed through UV−vis absorption, phosphorescent emission, and electrochemical measurements. Upon addition of Hg^{2+}, the obvious spectral blue-shifts in absorption and phosphorescent emission bands were measured for $Ir(btp)_2$(acac), which could be observed by the naked eye. Further investigation indicated that the interaction between Hg^{2+} and the sulfur of cyclometalated ligands is responsible for the significant variation in optical and electrochemical signals, which was also confirmed by density functional theory (DFT) calculation. It is the charge transfer from the iridium center to cyclometalated ligands that increases the electron density of cyclometalated ligands, which makes the coordination of sulfur to Hg^{2+} easier.

Introduction

Recently, phosphorescent heavy-metal complexes have been attracting more and more attention due to their high luminescence quantum yields and long-lived excited states.[1] The strong spin−orbit coupling caused by the heavy atom effect leads to an efficient intersystem crossing from the singlet (S_1) to the triplet (T_n) as well as the enhancement of the T_1-S_0 transition. Phosphorescent heavy-metal complexes have been explored for a multitude of photonic applications including organic light-emitting diodes,[2] photovoltaic cells,[3] biological labeling reagents,[4] and hydrogen production via the photoreduction of water.[5] Recently, the use of phosphorescent heavy-metal complexes as chemosensors has also attracted considerable interest,[6] due to the photophysical properties of heavy-metal complexes, such as emission wavelength shifts with changes in the local environment, significant Stokes shifts for easy separation of excitation and emission, and relatively long lifetimes compared to purely organic luminophores.[7] The relatively long lifetime can give heavy-metal complexes excellent temporal resolution and their luminescence can be easily separated from fluorescent backgrounds. Some heavy-metal complexes, such as platinum(II) complexes, rhenium(I) complexes, and ruthenium(II) complexes, have successfully been explored as phosphorescent chemosensors for anions,[8] oxygen concentration,[9] and metal ions.[6c] However, as one of the best phosphorescent dyes, iridium(III) complexes were scarcely used as chemosensors. Up to now, only a few cases of phosphorescent iridium(III) complexes were reported to sense oxygen[10] and Ca^{2+},[11] and no iridium(III) complexes were utilized to recognize transition- and heavy-metal ions.

Transition- and heavy-metal ions play an important role in many fundamental physiological processes in organisms; therefore, development of highly selective chemosensors for the detection of transition- and heavy-metal ions is very important. Among them, mercury is a dangerous and widespread global pollutant,[12a] and it causes serious environmental and health problems because marine aquatic organisms convert inorganic

* To whom correspondence should be addressed. Fax: 86-21-55664621. Tel: 86-21-55664185. E-mail: fyli@fudan.edu.cn (F.Y.L.); chhuang@pku.edu.cn (C.H.H.).

(1) (a) Lamansky, S.; Djurovich, P.; Murphy, D.; Abdel-Razzaq, F.; Lee, H. E.; Adachi, C.; Burrows, P. E.; Forrest, S. R.; Thompson, M. E. *J. Am. Chem. Soc.* **2001**, *123*, 4304−4312. (b) Zhu, W.; Mo, Y.; Yuan, M.; Yang, W.; Cao, Y. *Appl. Phys. Lett.* **2002**, *80*, 2045−2047. (c) Gong, X.; Ostrowski, J. C.; Bazan, G. C.; Moses, D.; Heeger, A. J. *Appl. Phys. Lett.* **2002**, *81*, 3711−3713. (d) Thomas, K. R. J.; Velusamy, M.; Lin, J. T.; Chien, C. H.; Tao, Y. T.; Wen, Y. S.; Hu, Y. H.; Chou, P. T. *Inorg. Chem.* **2005**, *44*, 5677−5685. (e) Chan, S. C.; Chan, M. C. W.; Wang, Y.; Che, C. M.; Cheung, K. K.; Zhu, N. *Chem.−Eur. J.* **2001**, *7*, 4180−4190. (f) Lu, W.; Mi, B. X.; Chan, M. C. W.; Hui, Z.; Che, C. M.; Zhu, N.; Lee, S. T. *J. Am. Chem. Soc.* **2004**, *126*, 4958−4971.

(2) (a) Tsuboyama, A.; Iwawaki, H.; Fururori, M.; Mukaide, T.; Kamatani, J.; Igawa, S.; Moriyama, T.; Miura, S.; Takiguchi, T.; Okada, S.; Hoshino, M.; Ueno, K. *J. Am. Chem. Soc.* **2003**, *125*, 12971−12979. (b) Adachi, C.; Baldo, M. A.; Thompson, M. E.; Forrest, S. R. *J. Appl. Phys.* **2001**, *90*, 5048−5051.

(3) (a) Wong, H. L.; Lam, L. S. M.; Cheng, K. W.; Man, K. Y. K.; Chan, W. K.; Kwong, C. Y.; Djurišić, A. B. *Appl. Phys. Lett.* **2004**, *84*, 2557−2559. (b) Hara, K.; Nishikawa, T.; Kurashige, M.; Kawauchi, H.; Kashima, T.; Sayama, K.; Aika, K.; Arakawa, H. *Sol. Energy Mater. Sol. Cells* **2005**, *85*, 21−30.

(4) (a) Lo, K. K. W.; Ng, D. C. M.; Chung, C. K. *Organometallics* **2001**, *20*, 4999−5001. (b) Lo, K. K. W.; Chan, J. S. W.; Lui, L. H.; Chung, C. K. *Organometallics* **2004**, *23*, 3108−3116.

(5) (a) Goldsmith, J. I.; Hudson, W. R.; Lowry, M. S.; Anderson, T. H.; Bernhard, S. *J. Am. Chem. Soc.* **2005**, *127*, 7502−7510. (b) Kirch, M.; Lehn, J. M.; Sauvage, J. P. *Helv. Chim. Acta* **1979**, *62*, 1345−1384. (c) Krishnan, C. V.; Brunschwig, B. S.; Creutz, C.; Sutin, N. *J. Am. Chem. Soc.* **1985**, *107*, 2005−2015.

(6) (a) de Silva, A. P.; Gunaratne, H. Q. N.; Gunnlaugsson, T.; Huxley, A. J. M.; McCoy, C. P.; Rademacher, J. T.; Rice, T. E. *Chem. Rev.* **1997**, *97*, 1515−1566. (b) Demas, J. N.; DeGraff, B. A. *Coord. Chem. Rev.* **2001**, *211*, 317−351. (c) Tang, W. S.; Lu, X. X.; Wong, K. M. C.; Yam, V. W. W. *J. Mater. Chem.* **2005**, *15*, 2714−2720.

(7) Carraway, E. R.; Demas, J. N.; DeGraff, B. A.; Bacon, J. R. *Anal. Chem.* **1991**, *63*, 337−342.

(8) Lin, Z. H.; Zhao, Y. G.; Duan, C. Y.; Zhang, B. G.; Bai, Z. P. *Dalton Trans.* **2006**, 3678−3684.

(9) Brinas, R. P.; Troxler, T.; Hochstrasser, R. M.; Vinogradov, S. A. *J. Am. Chem. Soc.* **2005**, *127*, 11851−11862.

(10) (a) Gao, R.; Ho, D. G.; Hernandez, B.; Selke, M.; Murphy, D.; Djurovich, P. I.; Thompson, M. E. *J. Am. Chem. Soc.* **2002**, *124*, 14828−14829. (b) Huynh, L.; Wang, Z.; Yang, J.; Stoeva, V.; Lough, A.; Manners, I.; Winnik, M. A. *Chem. Mater.* **2005**, *17*, 4765−4773.

(11) Ho, M. L.; Hwang, F. M.; Chen, P. N.; Hu, Y. H.; Cheng, Y. M.; Chen, K. S.; Lee, G. H.; Chi, Y.; Chou, P. T. *Org. Biomol. Chem.* **2006**, *4*, 98−103.

10.1021/om061031r CCC: $37.00
Publication on Web 03/09/2007

mercury into neurotoxic methylmercury, a potent neurotoxin that bioaccumulates through the food chain in the tissues of fish and marine mammals.[12b,c] Subsequent ingestion of methylmercury by humans is connected to DNA damage, mitosis impairment, and nervous system defects.[12d,e] Therefore, it is important to explore new methods for detection of Hg^{2+}. A number of Hg^{2+}-selective sensors have been devised by utilizing chromogenic,[13] fluorogenic,[14] and electrochemical[15] behaviors of the devised compound. However, multisignaling chemosensors for Hg^{2+} that are capable of both optical and electrochemical sensing are very few.[16] Herein, we are interested in developing a multisignaling probe based on iridium(III) complexes that exhibits a naked-eye observed change in phosphorescent emission upon addition of Hg^{2+} over other metal ions.

It is well known that the chemical structures of cyclometalated ligands (C^N ligands) can strongly affect the photophysical and electrochemical properties of iridium(III) complexes. When the cyclometalated ligands of iridium(III) complexes contain specific metal-coordinating elements, we reason that the presence of metal ions can lead to dramatic changes in the photophysical and electrochemical properties of complexes. Herein, an iridium(III) complex, $Ir(btp)_2(acac)$[1a] (see Scheme 1), containing sulfur atoms was synthesized to provide a mercury-coordinating element and could be used as a highly selective and multisignaling optical−electrochemical sensor for Hg^{2+}.

Experimental Section

Materials. Acetylacetone, 2-ethoxyethanol, 2-bromopyridine, 2-benzothienylboronic acid, and thianaphtlene (bt) were obtained from Acros. Mercury(II) perchlorate hydrate was obtained from Aldrich. $IrCl_3 \cdot 3H_2O$ and tetrakis(triphenylphosphine)palladium(0) ($Pd(PPh_3)_4$) were industrial products and used without further purification. According to previous literature,[1a] 2-(benzo[*b*]thiophen-2-yl)pyridine (btp) was easily synthesized via the Suzuki coupling reaction, using $Pd(PPh_3)_4$ and K_2CO_3 from 2-bromopyridine and 2-benzothienylboronic acid, and was characterized by ^1H NMR spectroscopy.

Scheme 1. Chemical Structures of $Ir(btp)_2(acac)$, btp, and bt.

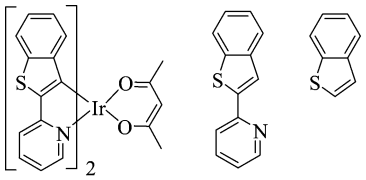

$Ir(btp)_2(acac)$ btp bt

General Experiments. ^1H NMR spectra were recorded with a Varian spectrometer at 400 MHz. Mass spectra were obtained on a Shimadzu matrix-assisted laser desorption/ionization time-of-flight mass spectrometer (MALDI-TOF-MS). The UV−visible spectra were recorded on a Shimadzu UV-2550 spectrometer. Steady-state emission experiments at room temperature were measured on an Edinburgh Instruments Xe-920 spectrometer. Lifetime studies were performed with an Edinburgh FL 920 photocounting system with a hydrogen-filled lamp as the excitation source. The data were analyzed by iterative convolution of the luminescence decay profile with the instrument response function using a software package provided by Edinburgh Instruments. The luminescence quantum yields of $Ir(btp)_2(acac)$ in air-equilibrated solution were measured with reference to rhodamine B ($\Phi_F = 0.69$ in ethanol).

Electrochemical Measurements. Electrochemical measurements were performed with an Eco Chemie Autolab. All measurements were carried out in a one-compartment cell under N_2 gas, equipped with a glassy-carbon working electrode, a platinum wire counter electrode, and a Ag/Ag^+ reference electrode. The supported electrolyte was a 0.10 mol L^{-1} dichloromethane solution of tetrabutyl ammonium hexafluorophosphate (Bu_4NPF_6). The scan rate was 50 $mV \cdot s^{-1}$.

Theoretical Calculations. The optimization of the complex structures was performed using B3LYP density functional theory. The LANL2DZ basis set was used to treat the iridium atom, whereas the 3-21G* basis set was used to treat all other atoms. The contours of the HOMO and LUMO orbitals were plotted.

Metal Cation Titration of $Ir(btp)_2(acac)$. Spectrophotometric titrations were performed on 20 μM solutions of $Ir(btp)_2(acac)$ in MeCN. Typically, aliquots of fresh cations (Ag^+, Cd^{2+}, Co^{2+}, Cr^{2+}, Cu^{2+}, Fe^{3+}, Mg^{2+}, Ni^{2+}, Pb^{2+}, Zn^{2+}, Hg^{2+}) were added, and the UV−vis absorption and fluorescent spectra of the samples were recorded.

Synthesis of $Ir(btp)_2(acac)$. Complex $Ir(btp)_2(acac)$ was synthesized according to previous literature.[1a] A mixture of 2-ethoxyethanol and water (3:1, v/v) was added to a flask containing $IrCl_3 \cdot 3H_2O$ (1 mmol) and btp (2.5 mmol). The mixture was refluxed for 24 h. After cooling, the red solid precipitate was filtered to give crude cyclometalated iridium(III) chloro-bridged dimer. To the mixture of crude chloro-bridged dimer (0.2 mmol) and Na_2CO_3 (1.4 mmol) were added 2-ethoxyethanol and acac (0.5 mmol), and then the slurry was refluxed for 12 h. After cooling to room temperature, a brown-red precipitate was collected by filtration and was chromatographed using CH_2Cl_2/petroleum ether (1:1, v/v) to give $Ir(btp)_2(acac)$, brown-red solid, yield 60%. ^1H NMR ($CDCl_3$, 400 MHz): δ 8.52 (d, $J = 5.6$ Hz, 2H), 7.85 (d, $J = 8.0$ Hz, 2H), 7.73 (t, $J = 7.8$ Hz, 2H), 7.55 (d, $J = 7.6$ Hz, 2H), 7.14 (t, $J = 5.6$ Hz, 2H), 6.82 (t, $J = 7.2$ Hz, 2H), 6.70 (t, $J = 7.2$ Hz, 2H), 6.27 (d, $J = 8.0$ Hz, 2H), 5.21 (s, 1H), 1.78 (s, 6H).

Results and Discussion

UV−Vis Absorption Spectroscopy. The absorption spectrum of $Ir(btp)_2(acac)$ in CH_3CN is shown in Figure 1. The complex

(12) (a) U.S. EPA, Regulatory Impact Analysis of the Clean Air Mercury Rule: *EPA-452/R-05-003*, 2005. (b) Boening, D. W. *Chemosphere* **2000**, *40*, 1335−1351. (c) Harris, H. H.; Pickering, I. J.; George, G. N. *Science* **2003**, *301*, 1203−1203. (d) Tchounwou, P. B.; Ayensu, W. K.; Ninashvili, N.; Sutton, D. *Environ. Toxicol.* **2003**, *18*, 149−175. (e) Clarkson, T. W.; Magos, L.; Myers, G. J. *N. Engl. J. Med.* **2003**, *349*, 1731−1737.

(13) (a) Zheng, H.; Qian, Z. H.; Xu, L.; Yuan, F. F.; Lan, L. D.; Xu, J. G. *Org. Lett.* **2006**, *8*, 859−861. (b) Tatay, S.; Gavina, P.; Coronado, E.; Palomares, E. *Org. Lett.* **2006**, *8*, 3857−3860. (c) Descalzo, A. B.; Martinez-Manez, R.; Radeglia, R.; Rurack, K.; Soto, J. *J. Am. Chem. Soc.* **2003**, *125*, 3418−3419. (d) Ros-Lis, J. V.; Marcos, M. D.; Martinez-Manez, R.; Rurack, K.; Soto, J. *Angew. Chem., Int. Ed.* **2005**, *44*, 4405−4407. (e) Cheng, Y. F.; Zhao, D. T.; Zhang, M.; Liu, Z. Q.; Zhou, Y. F.; Shu, T. M.; Li, F. Y.; Yi, T.; Huang, C. H. *Tetrahedron Lett.* **2006**, *47*, 6413−6416.

(14) (a) Song, K. C.; Kim, J. S.; Park, S. M.; Chung, K. C.; Ahn, S.; Chang, S. K. *Org. Lett.* **2006**, *8*, 3413−3416. (b) Yang, Y. K.; Yook, K. J.; Tae, J. *J. Am. Chem. Soc.* **2005**, *127*, 16760−16761. (c) Chae, M. Y.; Czarnik, A. W. *J. Am. Chem. Soc.* **1992**, *114*, 9704−9705. (d) Hennrich, G.; Sonnenschein, H.; Resch-Genger, U. *J. Am. Chem. Soc.* **1999**, *121*, 5073−5074. (e) Prodi, L.; Bargossi, C.; Montalti, M.; Zaccheroni, N.; Su, N.; Bradshaw, J. S.; Izatt, R. M.; Savage, P. B. *J. Am. Chem. Soc.* **2000**, *122*, 6769−6770. (f) Sakamoto, H.; Ishikawa, J.; Nakao, S.; Wada, H. *Chem. Commun.* **2000**, 2395−2396. (g) Nolan, E. M.; Lippard, S. J. *J. Am. Chem. Soc.* **2003**, *125*, 14270−14271. (h) Guo, X.; Qian, X.; Jia, L. *J. Am. Chem. Soc.* **2004**, *126*, 2272−2273. (i) Liu, B.; Tian, H. *Chem. Commun.* **2005**, 3156−3158. (j) Mello, J. V.; Finney, N. S. *J. Am. Chem. Soc.* **2005**, *127*, 10124−10125. (k) Nolan, E. M.; Lippard, S. J. *J. Mater. Chem.* **2005**, *15*, 2778−2783. (l) Rurack, K.; Kollmannsberger, M.; Resch-Genger, U.; Daub, J. *J. Am. Chem. Soc.* **2000**, *122*, 968−969. (m) Huang, C. C.; Chang, H. T. *Anal. Chem.* **2006**, *78*, 8332−8338. (n) Zhu, X. J.; Fu, S. T.; Wong, W. K.; Guo, J. P.; Wong, W. Y. *Angew. Chem., Int. Ed.* **2006**, *45*, 3150−3154. (o) Yang, Y. K.; Yook, K. J.; Tae, J. *J. Am. Chem. Soc.* **2000**, *127*, 16760−16761.

(15) Lloris, J. M.; Martínez-Máñez, R.; Padilla-Tosta, M. E.; Pardo, T.; Soto, J.; Beer, P. D.; Cadman, J.; Smith, D. K. *J. Chem. Soc., Dalton Trans.* **1999**, 2359−2370.

(16) Jiménez, D.; Martínez-Máñez, R.; Sancenón, F.; Soto, J. *Tetrahedron Lett.* **2004**, *45*, 1257−1259.

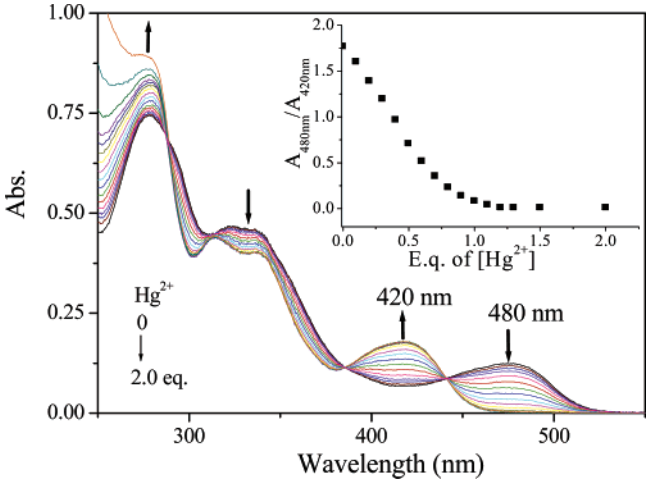

Figure 1. Changes in the UV−vis absorption spectra of $Ir(btp)_2$(acac) (20 μM) in CH_3CN solution with various amounts of Hg^{2+} ions (0−40 μM). Inset: titration curve of $Ir(btp)_2$(acac) with Hg^{2+}.

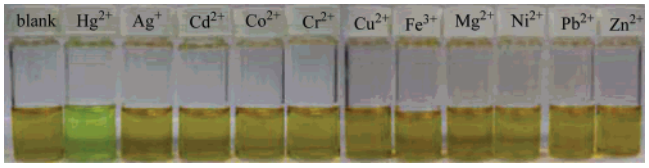

Figure 2. Color variation observed in CH_3CN solutions of $Ir(btp)_2$(acac) (500 μM) in the presence of 1 equiv of certain metal cations.

displays intense absorption bands in the ultraviolet region of 280−400 nm with extinction coefficients (ϵ) of $\sim 10^5$ $mol^{-1}\cdot L\cdot cm^{-1}$, which are assigned to the spin-allowed singlet ligand-centered (^{1}LC) transitions. The weak band at 480 nm with the extinction coefficient ϵ of 6.1×10^3 $mol^{-1}\cdot L\cdot cm^{-1}$ is assigned to a singlet metal-to-ligand charge transfer (^{1}MLCT) transition. The addition of increasing amounts of Hg^{2+} to the solution of $Ir(btp)_2$(acac) promoted some changes in its absorption spectrum. The absorbance at 480 nm decreased gradually, whereas a new band at 420 nm appeared (Figure 1), corresponding to a λ_{max}(abs) blue-shift of 60 nm with two isobestic points at 440 and 385 nm, which induced a color change from orange to yellow-green (see Figure 2), indicating that $Ir(btp)_2$(acac) can serve as a sensitive "naked-eye" indicator for Hg^{2+}. As shown in the Figure 1 inset, metal-binding titrations indicate that $Ir(btp)_2$(acac) forms a 1:1 complex with Hg^{2+}. The extinction coefficient ϵ of the band at 420 nm after the addition of 1 equiv of Hg^{2+} is 8.5×10^3 $mol^{-1}\cdot L\cdot cm^{-1}$. The binding constant value (K) calculated from absorption titration data is 1.5×10^4 M^{-1}.

Fluorimetric Response of Complex $Ir(btp)_2$(acac) to Hg^{2+}. It is well known that fluorescent emission spectroscopy is more sensitive toward small changes that affect the electronic properties of molecular receptors.[14] Herein, the complexation ability of $Ir(btp)_2$(acac) with Hg^{2+} was also investigated by photoluminescent technique. The luminescence spectra of complex $Ir(btp)_2$(acac) in the absence and presence of Hg^{2+} are shown in Figure 3. In CH_3CN solution, $Ir(btp)_2$(acac) showed an intense emission band at 610 nm with a shoulder band at 660 nm and the photoluminescent color is deep red. The luminescent quantum yield of $Ir(btp)_2$(acac) in air-equilibrated solution was 0.026. The emission lifetimes monitored at 610 and 660 nm in air-equilibrated solution at room temperature were measured to be 137.9 and 136.5 ns, respectively, indicating the phosphorescent emission nature of $Ir(btp)_2$(acac). The similar lifetimes show that a single species was responsible for the luminescence.

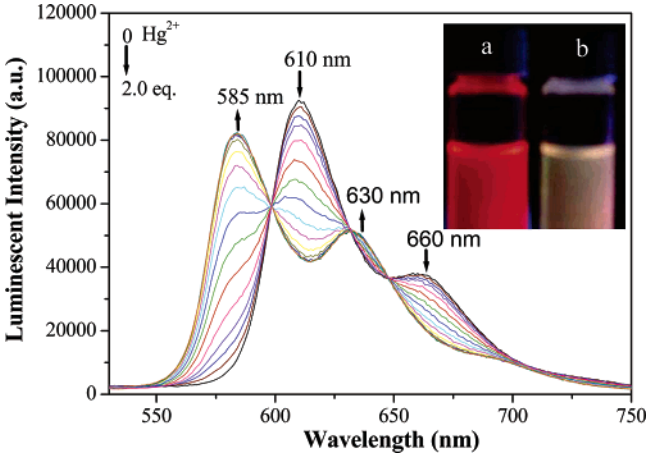

Figure 3. Changes in the luminescence spectra of $Ir(btp)_2$(acac) (20 μM) in air-equilibrated CH_3CN solution with various amounts of Hg^{2+} ions (0−40 μM) (λ_{ex} = 440 nm). λ_{ex} = 440 nm. Inset: Emission color observed in CH_3CN solution of $Ir(btp)_2$(acac) (500 μM) in the absence (a) and presence (b) of 1 equiv of Hg^{2+}.

The excitation spectra monitoring these two emission bands were similar (see Figure S1 in the Supporting Information), indicating that they came from the same excited states. Upon addition of Hg^{2+}, the intensity of these two bands decreased and two new bands at 585 and 630 nm appeared gradually, corresponding to a blue-shift of about 30 nm with three isoemissive points at 647, 632, and 598 nm. The emission color was changed from deep red to orange (see Figure 3, inset), which could be observed by the naked eye. The luminescent quantum yield of $Ir(btp)_2$(acac) in the prescence of 1 equiv of Hg^{2+} in air-equilibrated solution was 0.027. Moreover, the emission lifetimes monitored at 585 and 630 nm in air-equilibrated solution at room temperature were also measured to be 275.9 and 273.8 ns, respectively. Such long lifetimes in air-equilibrated solution show that the emitting states of $Ir(btp)_2$(acac) in the presence of Hg^{2+} also have triplet character, and the similar lifetimes also show that a single species was responsible for the luminescence. The excitation spectra monitoring these two new bands were similar (see Figure S2 in the Supporting Information), but were significantly different from those of pure $Ir(btp)_2$(acac) monitored at 610 and 660 nm. The differences in the excitation and absorption spectra coupled with the different emission spectra in the absence and presence of Hg^{2+} show that a different ground-state species is responsible for each of the two different emissions. Coupled with the different single-exponential decay times, there is no interconversion between the two forms during the excited-state decay. By the changes in the fluorimetric response of $Ir(btp)_2$(acac) in the presence of varying concentrations of Hg^{2+}, the stoichiometry of the complex system was also determined to be 1:1, indicating the formation of a 1:1 complex, which is in agreement with the result obtained from the UV−vis absorption technique. Furthermore, at the concentration of the complex employed in our studies, Hg^{2+} could be detected down to a concentration of 10^{-7} M, that is, at concentrations in the ppb range, which is comparable with many previous reports.[14m,o,18]

Electrochemical Studies. To explore further the utility of $Ir(btp)_2$(acac) as an electrochemical sensor for Hg^{2+}, cyclic voltammetry (CV) studies were conducted in CH_3CN solution.

(17) Pearson, R. G. *J. Am. Chem. Soc.* **1963**, *85*, 3533−3539.
(18) Coronado, E.; Galán-Mascarós, J. R.; Marti-Gastaldo, C.; Palomares, E.; Durrant, J. R.; Vilar, R.; Gratzel, M.; Nazeeruddin, M. K. *J. Am. Chem. Soc.* **2004**, *127*, 12351−12356.

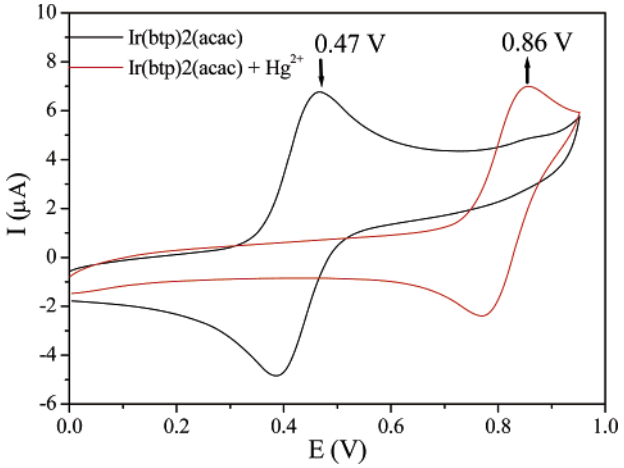

Figure 4. Cyclic voltammograms of $Ir(btp)_2(acac)$ (500 μM) in CH_3CN solution in the absence and presence of 1 equiv of Hg^{2+} ions. Inset: Electrochemical titration of $Ir(btp)_2(acac)$ with Hg^{2+}.

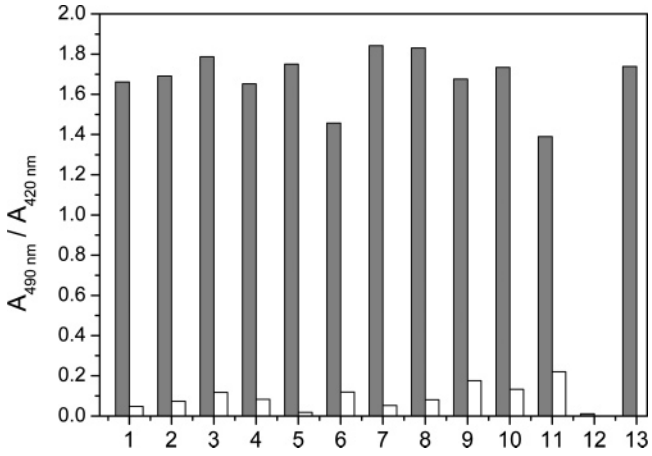

Figure 5. Absorption response of $Ir(btp)_2(acac)$ (20 μM) in the presence of various metal cations (1 equiv) in MeCN solution. Bars represent the ratio ($A_{490\ nm}/A_{420\ nm}$) of absorbance intensity at 490 and 420 nm. Solid bars represent the addition of 1-fold various metal cations to a 20 μM solution of $Ir(btp)_2(acac)$. White bars represent the $A_{490\ nm}/A_{420\ nm}$ ratio after addition of Hg^{2+} (20 μM) to the above solution. 1, Ag^+; 2, Cd^{2+}; 3, Co^{2+}; 4, Cr^{2+}; 5, Cu^{2+}; 6, Fe^{3+}; 7, Mg^{2+}; 8, Ni^{2+}; 9, Pb^{2+}; 10, Zn^{2+}, 11, the mixture of 1−10; 12, Hg^{2+}; 13, without metal cation.

A reversible oxidation wave at 0.47 V can be observed for $Ir(btp)_2(acac)$ in the absence of Hg^{2+}. According to the previous electrochemical studies on iridium(III) complexes, this oxidation wave is assigned to a metal-centered Ir^{III}/Ir^{IV}oxidation process. The addition of increasing amounts of Hg^{2+} to a solution of $Ir(btp)_2(acac)$ caused a significant modification in the cyclic voltammetry (Figure 4 and Figure S5 in the Supporting Information). The intensity of the oxidation wave at 0.47 V decreased and a new reversible oxidation wave at 0.86 V appeared with progressive addition of Hg^{2+}. The saturation behavior of the intensity of the oxidation wave at 0.86 V after the addition of 1.0 equiv of Hg^{2+} also reveals that the complex system has a 1:1 stoichiometry.

Selective Optical Response of Complex $Ir(btp)_2(acac)$ to Various Metal Ions. For an excellent chemosensor, high selectivity is a matter of necessity. Herein, the selective coordination studies of $Ir(btp)_2(acac)$ by absorption spectroscopy were then extended to related heavy, transition, and main group metal ions in CH_3CN solution. As shown in Figure 5, only the addition of Hg^{2+} resulted in a prominent absorption change,

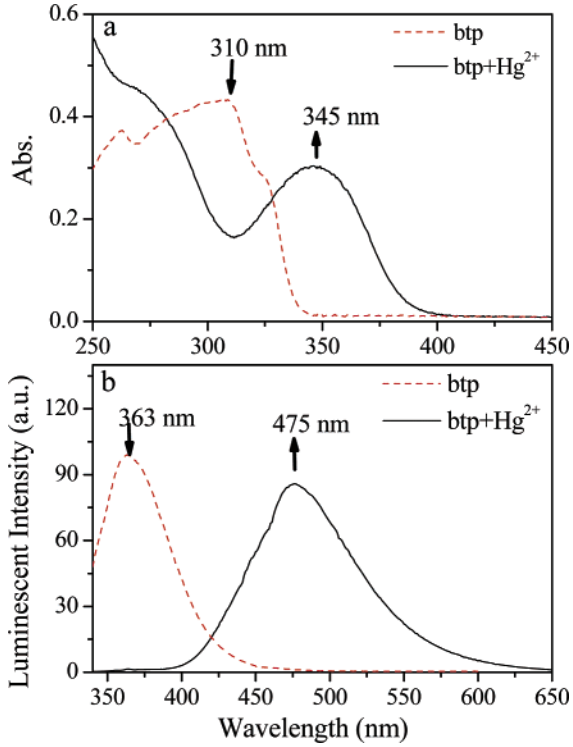

Figure 6. UV−vis absorption (a) and luminescence spectra (b) of btp (20 μM in CH_3CN) in the absence and prescence of 1 equiv of Hg^{2+}. λ_{ex} = 263 nm.

whereas very weak variations of absorption spectra of $Ir(btp)_2(acac)$ were observed upon addition of an excess of the other metal ions, such as Mg^{2+}, Cr^{2+}, Fe^{3+}, Co^{2+}, Ni^{2+}, Pb^{2+}, Ag^+, Zn^{2+}, Cu^{2+}, and Cd^{2+}. Therefore, $Ir(btp)_2(acac)$ displayed a high selectivity in sensing Hg^{2+}. Similarly, achieving high selectivity for the analyte of interest over a complex background of potentially competing species is challenge in sensor development. Thus, the competition experiment was also carried out by adding Hg^{2+} to the solutions of $Ir(btp)_2(acac)$ in the presence of other metal ions. As shown in Figure 5, whether in the absence or presence of the other metal ions, obvious spectral changes were observed for $Ir(btp)_2(acac)$ upon addition of Hg^{2+}. The results indicate that the sensing of Hg^{2+} by $Ir(btp)_2(acac)$ is hardly affected by these commonly coexistent ions.

Furthermore, selective and competition experiments were also carried out by luminescent spectra (see Figure S6 in the Supporting Information). The results also showed the high selectivity for Hg^{2+} in the prescence of other metal ions. The addition of some other metal ions, such as Pb^{2+} and Cd^{2+}, induced the decrease of the emission band at 610 nm. It appears that there may be bimolecular quenching of the excited state. The Stern−Volmer (SV) fluorescence quenching plots for Pb^{2+} and Cd^{2+} are shown in Figure S7, and the values of SV quenching constants (K_{sv}) for Pb^{2+} and Cd^{2+} are 3.1×10^2 and 1.1×10^3, respectively.

Mechanism of Complex $Ir(btp)_2(acac)$ in Sensing Hg^{2+}. From the above discussion, we can see that the photophysical and electrochemical properties of complex $Ir(btp)_2(acac)$ can be changed significantly by the addition of Hg^{2+}. It is well known that soft Hg^{2+} ions (*soft acid*) can preferentially interact with sulfur (*soft base*) according to Pearson's hard and soft acids and bases theory.[17] In a previous report, Palomares et al. have found that the coordination of Hg^{2+} to a sulfur atom induces a color change for ruthenium complexes.[18] So, we can deduce that the significant variations in the photophysical and electro-

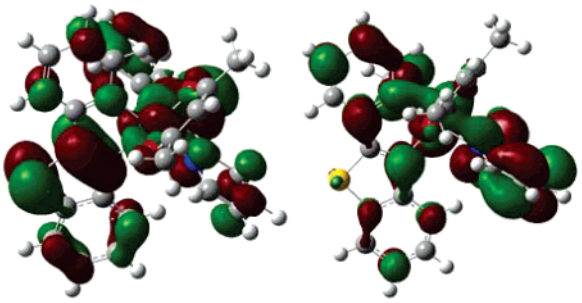

Figure 7. HOMO (left) and LUMO (right) distributions of $Ir(btp)_2(acac)$.

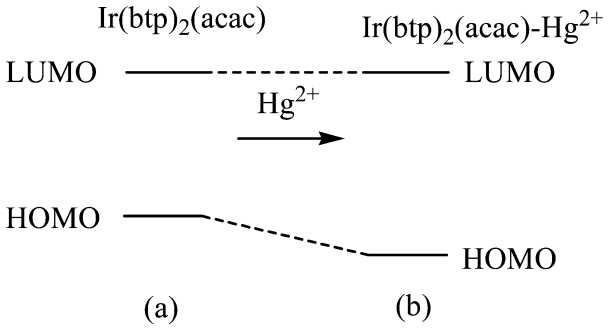

Figure 8. Variation in HOMO and LUMO energy levels of $Ir(btp)_2(acac)$ in the absence (a) and presence (b) of Hg^{2+}.

chemical properties of complex $Ir(btp)_2(acac)$ are induced by coordination of Hg^{2+} to the lone-pair electrons on the sulfur atom of cyclometalated ligands of the complex $Ir(btp)_2(acac)$.

There is a possibility that $Ir(btp)_2(acac)$ may decompose by the addition of Hg^{2+} and the complex Hg-btp is formed, which is responsible for the significant change of photophysical and electrochemical properties. Hence, the coordination of the ligand btp with Hg^{2+} was also investigated by spectral techniques. The absorption and luminescence spectra of btp in the absence and prescence of 1 equiv of Hg^{2+} are shown in Figure 6. Upon addition of Hg^{2+}, the absorption maximum of btp was shifted from 310 to 345 nm and the luminescent emission peak was also shifted from 363 to 475 nm. The emission lifetime monitored at 475 nm, corresponding to the emission of complex Hg-btp, was 1.1 ns. The data of absorption and luminescence properties of Hg-btp are significantly different from those of $Ir(btp)_2(acac)$-Hg. Hence, the possibility of decomposition for $Ir(btp)_2(acac)$ after the addition of Hg^{2+} can be excluded.

In addition, we investigated the response of UV−vis absorption of the compound thianaphthene (bt, see Scheme 1), which is a fragment of the ligand btp containing sulfur, to various amounts of Hg^{2+} (see Figure S8 in the Supporting Information). No obvious change was observed, indicating no (or very weak) interaction between the sulfur of bt and Hg^{2+}. Considering the same benzothienyl fragment for $Ir(btp)_2(acac)$ and bt, the difference of response to Hg^{2+} can be ascribed to the formation of the iridium(III) complex.

For a better understanding of the influence of Hg^{2+} on the photophysical and electrochemical properties of $Ir(btp)_2(acac)$, the HOMO and LUMO distributions of $Ir(btp)_2(acac)$ were calculated by density functional theory (DFT). As shown in Figure 7, the HOMO primarily resides on the iridium center and benzothienyl part of the cyclometalated ligands and the LUMO primarily resides on the pyridyl part of the cyclometalated ligands, which are similar to most iridium(III) complexes.[19] Hence, the coordination of Hg^{2+} to the sulfur atom can significantly influence the HOMO energy level, whereas the influence on the LUMO energy level is negligible. The coordination of Hg^{2+} to the sulfur atom reduces the electron density on the benzothienyl part of the cyclometalated ligand and lowers the electron-donating ability of the cyclometalated ligand, and then the electron density on the iridium center is also reduced. As a result, the HOMO energy level is lowered and the energy gap between the HOMO and LUMO is increased, leading to the remarkable blue-shift in the absorption and luminescence spectra. Such changes of energy levels for $Ir(btp)_2(acac)$ are illustrated in Figure 8. In addition, the decrease of electron density on the iridium center also makes the Ir^{III}/Ir^{IV}oxidation process more difficult and the corresponding oxidation wave is shifted positively.

Conclusions

In summary, we have presented a highly selective and multisignaling optical−electrochemical chemosensor for Hg^{2+} based on the phosphorescent iridium(III) complex $Ir(btp)_2(acac)$. Especially, the complex shows a naked-eye phosphorescent change in the Hg^{2+} ion over other metal cations. The interaction between Hg^{2+} and the sulfur atom of cyclometalated ligands is responsible for the significant variations in optical and electrochemical signals. To the best of our knowledge, this is the first report of a chemosensor for transition- and heavy-metal ions based on a phosphorescent iridium(III) complex. Due to the poor solubility of the complex in water, the analysis is in a nonaqueous media and probably only good for ionic Hg^{2+}. However, this preliminary understanding of the Hg^{2+} sensing mechanism would actually help to design a series of new phosphorescent probes based on iridium(III) complexes by simply modifying the chemical structures of the ligands to contain specific coordinating elements and explore the new application in chemosensors for iridium(III) complexes as the best phosphorescent dye.

Acknowledgment. The authors are thankful for the financial support from National Natural Science Foundation of China (20490210 and 20501006), National High Technology Program of China (2006AA03Z318), Shanghai Science and Technology Community (05DJ14004 and 06QH14002), and Huo Yingdong Education Foundation (104012).

Supporting Information Available: Excitation spectra of $Ir(btp)_2(acac)$ before and after addition of Hg^{2+}. UV−vis and fluorescence spectra upon titration with other metal caions. Selective fluorimetric response of complex $Ir(btp)_2(acac)$ to various metal caions. This material is available free of charge via the Internet at http://pubs.acs.org.

OM061031R

(19) (a) Hwang, F. M.; Chen, H. Y.; Chen, P. S.; Liu, C. S.; Chi, Y.; Shu, C. F.; Wu, F. I.; Chou, P. T.; Peng, S. M.; Lee, G. H. *Inorg. Chem.* **2005**, *44*, 1344−1353. (b) Li, J.; Djurovich, P. I.; Alleyne, B. D.; Yousufuddin, M.; Ho, N. N.; Thomas, J. C.; Peters, J. C.; Bau, R.; Thompson, M. E. *Inorg. Chem.* **2005**, *44*, 1713−1727.